J Solid State Electrochem (2007) 11:737–743
DOI 10.1007/s10008-006-0210-3

ORIGINAL PAPER

Magnetic field effects on microstructural variation of electrodeposited cobalt films

Hisayoshi Matsushima · Adriana Ispas · Andreas Bund · Waldfried Plieth · Yasuhiro Fukunaka

Received: 26 June 2006 / Accepted: 8 August 2006 / Published online: 11 October 2006

Abstract The electrodeposition process of Co films in a sulfuric acid solution was examined in a magnetic field (0–5 T). The surface morphology of Co films electrodeposited without a magnetic field was drastically modified with the variation of hydrogen gas evolution rate. Crystalline α-Co was formed in the range of pH=1.5–6.0, while β-Co was not observed. When the magnetic field was superimposed perpendicular to the electric field in the acidic solution (pH=1.5), the hydrogen evolution rate was promoted by MHD convection, which enhanced the ionic mass transfer (H^+ and Co^{2+}) near the electrode surface. Moreover, crystalline β-Co was formed simultaneously with the appearance of the elongated ridge-shape precipitates under a higher magnetic field (≥3 T).

Keywords Cobalt electrodeposition · Magnetic field · Surface morphology · β-Cobalt · MHD convection

Introduction

The concept of electrochemical processing of tailored materials has been widely accepted even in the field of microelectronics industry. This is because electrochemical processing can continuously control the film microstructure on a large scale more easily than sputtering or physical vapor methods. Thus, it provides a much higher productivity. Many international symposiums have been organized for "tailored materials" [1–3].

Magnetic layers have been utilized in many applications as data storage devices and sensors. Cobalt is particularly one of the most attractive ferromagnetic materials. The microstructural variation plays an essential role to control the magnetic properties, as reported in recent papers [4, 5].

Electrochemical processing is frequently characterized as nonequilibrium materials processing. In the field of nonequilibrium materials science, the advancement of the superconducting technology has opened unique aspects for electrochemical reactions by applying high magnetic field. Magnetohydrodynamic (MHD) convection is considered as one of the characteristic phenomena in magnetro-electrochemical processes. The convection is induced by the electromagnetic interaction (Lorenz force), $J \times B$, where J is the Faraday current density and B is the magnetic flux density. It is well known that the convection enhances the ionic mass transfer rate to increase the deposition current [6–9].

Moreover, a magnetic field remarkably influences the microstructural properties [10–14]. In our previous works [15–17], the microstructural variation of electrodeposited iron film has been investigated under MHD flow conditions. The surface morphology changes into roundish and finer precipitates, depending on the direction of the magnetic field. The texture formation drastically changes from uniaxial to biaxial growth by the convection, which probably influences the surface pH value.

Some papers have been dealing with the correlation between cobalt deposition parameters (pH, current density, and temperature) and magnetic properties (coercivity and

Contribution to special issue "Magnetic field effects in Electrochemistry"

H. Matsushima (✉) · A. Ispas · A. Bund · W. Plieth
Institute of Physical Chemistry and Electrochemistry,
Dresden University of Technology,
01062 Dresden, Germany
e-mail: h.matsushima@chemie.tu-dresden.de

Y. Fukunaka
Department of Energy Science and Technology,
Graduate School of Energy Science, Kyoto University,
Sakyo-ku, Kyoto 606-8501, Japan

hysteresis loop) [18–21]. Armyanov [4] reviews that the comprehension between the cobalt deposition condition and the electrocrystallization mechanism helps reasonably tailoring the interface microstructure to induce unique magnetic properties.

During the electrocrystallization process, cobalt metal is formed not only in hexagonal closed packed (α-Co), but also in face centered cubic (β-Co) structure, which is the thermodynamically stable phase above 417 °C. Vicenzo and Cavallotti [22] have systematically investigated the cobalt crystal growth under various deposition conditions. It has been confirmed that β-Co is formed in a low-pH solution and suggested that the hydrogen adsorption phenomena are deeply related to the β-Co formation mechanism [23–25]. However, much more investigation is still necessary to clarify the mechanism.

In this work, cobalt films are galvanostatically electrodeposited from cobalt sulfate electrolyte solutions over a wide range of pH values without a magnetic field. Then, the microstructural variations and the formation of β-cobalt in a magnetic field are studied by SEM and X-ray diffraction (XRD) measurements.

Experimental

The electrochemical measurements were carried out with a three-electrode system as illustrated in Fig. 1. The electrode assembly was composed of a short rectangular channel ($10\times10\times30$ mm^3, polystyrene) with two open ends (top and bottom). The channel cell was vertically immersed in a 350-ml electrolytic bath. The cathode was a sheet of copper ($5\times5\times0.3$ mm^3). The anode was a cobalt film electrodeposited from 1.0 M $CoSO_4$ solution. The copper substrate was cleaned with HNO_3 solution and rinsed with acetone. The reference electrode was a Ag/AgCl electrode in a saturated KCl aqueous solution.

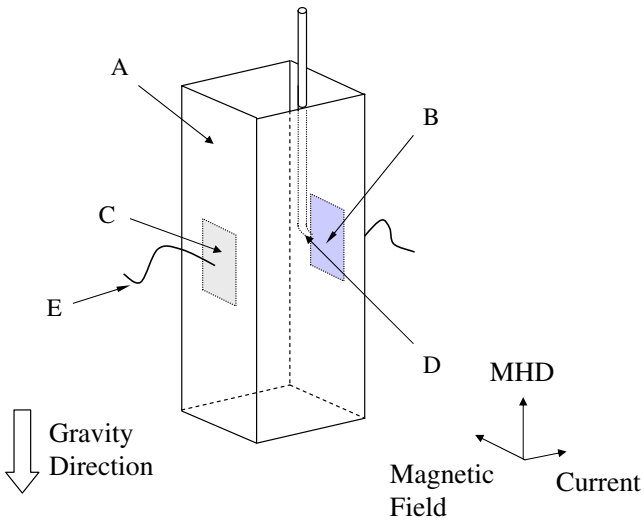

Fig. 1 Schematic diagram of the electrolytic cell. **a** Plastic cell ($10\times10\times30$ mm), **b** working electrode (Cu, $5\times5\times0.3$ mm), **c** counter electrode (Co, $3\times5\times0.3$ mm), **d** Luggin probe (ϕ=0.5 mm), **e** contacting wires

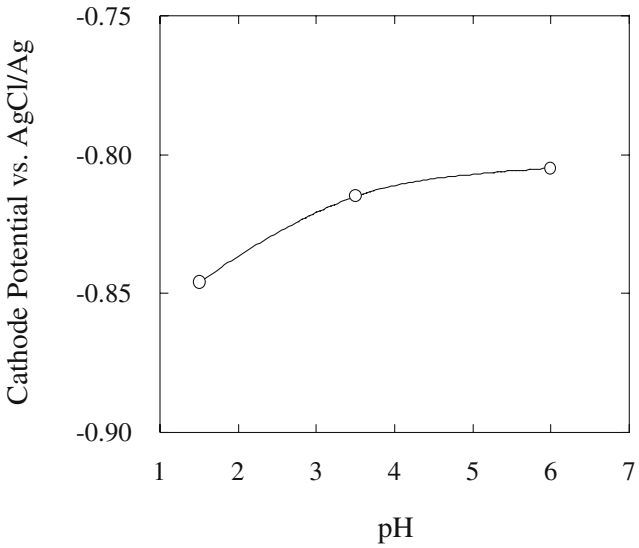

Fig. 2 Cathode potential measured in various pH electrolyte solutions during cobalt electrodeposition at 10 mA cm^{-2} (electrolyte: 1.65 M $CoSO_4$, 0.35 M $CoCl_2$, 0.38 M H_3BO_3)

The electrolyte compositions were 1.65 M $CoSO_4$, 0.35 M $CoCl_2$, and 0.38 M H_3BO_3, and the temperature was maintained at 298 K. The present study focused on three values of the pH (pH=1.5, 3.5, and 6.0). We consider that the electrodeposition process is more complicated over a wider range of the pH value. For example, colloidal cobalt hydroxide is formed in solutions with higher pH.

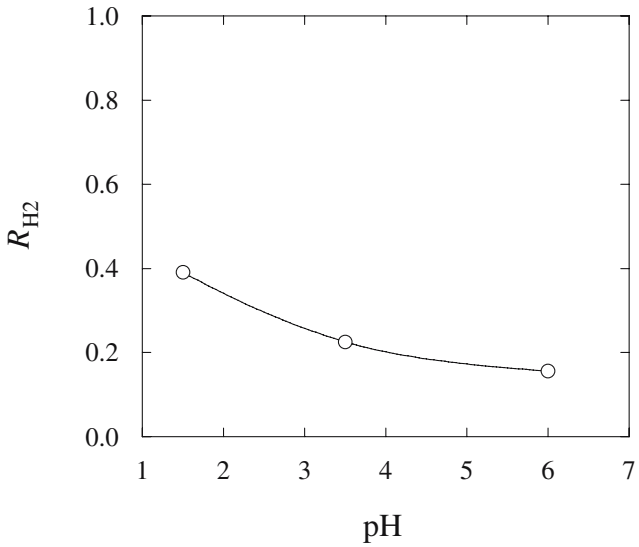

Fig. 3 Ratio of the hydrogen partial current to the total current, R_{H2}, measured in various pH electrolyte solutions during cobalt electrodeposition at 10 mA cm^{-2} (electrolyte: 1.65 M $CoSO_4$, 0.35 M $CoCl_2$, 0.38 M H_3BO_3)

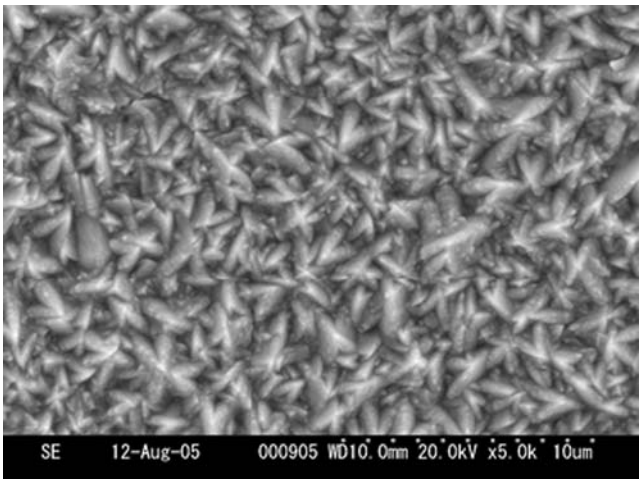

(a)

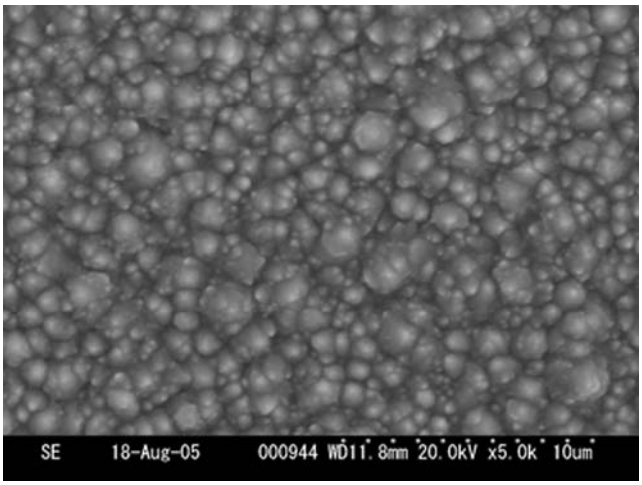

(b)

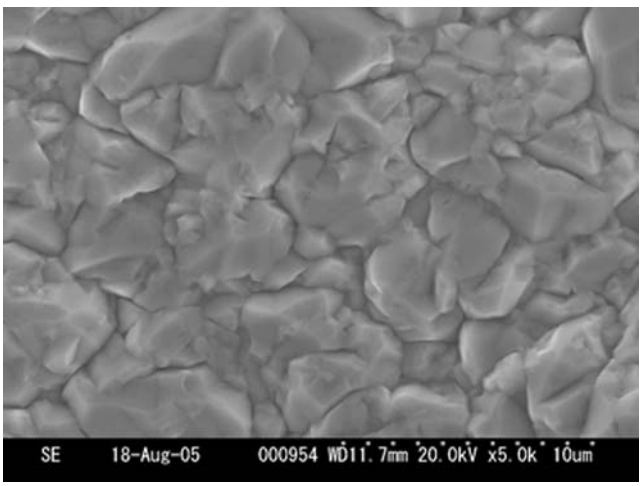

(c) 5 μm

◀ **Fig. 4** SEM images of the cobalt surface morphology electrodeposited at 10 mA cm^{-2} with 150 C cm^{-2} [pH=1.5 (**a**), 3.5 (**b**), and 6.0 (**c**)]

The colloidal particles probably influence the film microstructure, which would make it difficult to study the magnetic field effect.

The electrodeposition was conducted galvanostatically at 10 mA cm^{-2}. To reduce the effects from the copper substrate on the preferential growth process of cobalt, a thick cobalt film was electrodeposited. The amount of electricity was maintained at 150 C cm^{-2}, which corresponds roughly to an average cobalt film thickness of 15 to 50 μm depending on the current efficiency.

A static and uniform magnetic field was generated by a superconducting magnet (HF5-100VHF, Sumitomo Heavy Industry). It was superimposed vertically to the electric field so that upward MHD convection was introduced as shown in Fig. 1. The surface morphology was observed by scanning electron microscopy (S-2600H, Hitachi) and the crystal structure was analyzed by XRD pattern (Multiflex, Rigaku, 40 kV, 40 mA).

Results and discussion

pH Effects

Figure 2 shows the deposition potential measured in various pH solutions. It slightly shifts towards the anodic direction with increasing the pH value and tends to saturate at higher values.

Hydrogen gas simultaneously evolves with the cobalt precipitation reaction because the equilibrium potential of H^+/H is more anodic than that of Co^{2+}/Co. The ratio of the hydrogen partial current to the total one, R_{H2}, was calculated from the weight change of the substrate. Figure 3 shows the dependence of H_2 gas evolution rate on pH value. It apparently decreases from 0.4 to 0.16 with increasing pH. This can be explained by the surface concentration of H^+ ions. Because the H^+ concentration is lower at higher pH, the hydrogen evolution potential shifts to more cathodic values.

The electrodeposition was interrupted at 150 C cm^{-2}, and the surface morphology was observed by SEM. Figure 4 illustrates that the surface morphology of the electrodeposits drastically varies with pH value, as reported in some papers [5, 26]. At pH 1.5, the pyramidal-shaped deposits appear with a size of about 4 μm. At pH 3.5, the electrode surface is covered with roundish deposits. The average grain size is 3 μm, and the variance of the size distribution function seems to be relatively wide. At pH 6.0, precipitate coarsening further progresses and a flattened

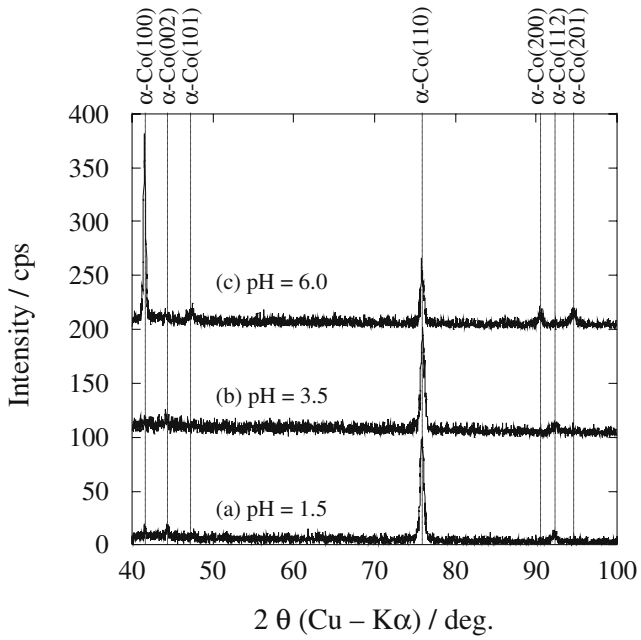

Fig. 5 XRD patterns of the cobalt film electrodeposited at 10 mA cm^{-2} in various pH electrolyte solutions, pH=1.5 (**a**), 3.5 (**b**), and 6.0 (**c**)

surface of the deposits is observed. The average size of 7 μm is much larger than the other electrodeposits at pH 1.5 and 3.5. The appearance of faceted grains with pyramidal shapes at lower pH might be explained by the significant evolution rate of hydrogen gas bubbles as seen in Fig. 3. That is, the cobalt deposits may grow larger without any macroscopic blocks by the bubbles sticking on the electrode.

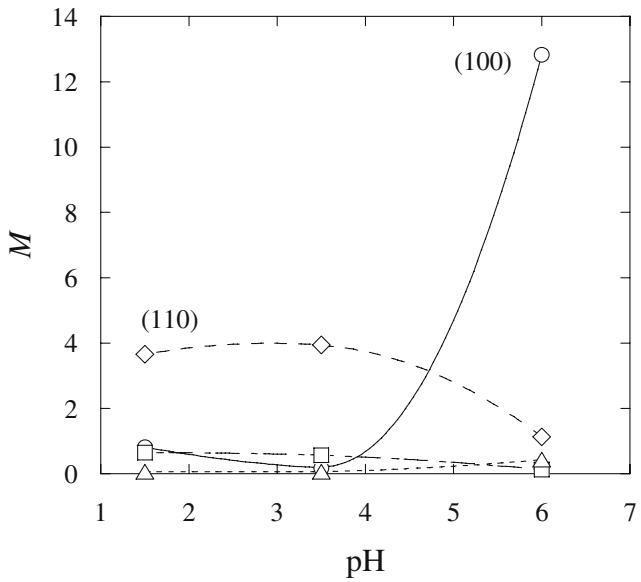

Fig. 6 Dependence of orientation index, *M*, on the electrolyte pH value for cobalt films electrodeposited without a magnetic field [*circles* (100) plane, *squares* (002) plane, *diamonds* (110) plane, and *triangles* (201) plane]

Table 1 Calculated surface pH values, pH^S, at 10 mA cm^{-2} without a magnetic field

pH	Values		
pH^b	1.5	3.5	6.0
pH^S	1.8	7.8	7.7

The crystal structure was analyzed by XRD as shown in Fig. 5. Then, the orientation index, *M*, was calculated to demonstrate the pH dependence (Fig. 6). α-Co(110) was preferentially oriented at both pH 1.5 and 3.5 and suppressed at pH 6.0. Although the surface morphology considerably changed between Fig. 4a and b, such a significant variation was not found in the pH dependence of the orientation index in the present results.

On the other hand, the strongest peak corresponding to α-Co(100) appears at pH 6.0. It suggests that the precipitated α-Co crystals rotate around the c-axis from the (110) to the (100) plane, which is energetically much more stable. It has been reported that the hydroxide adsorption depends on the crystal plane [22]. The surface pH value was estimated by the measured hydrogen gas evolution rate. For the details of the calculation, the reader is referred to Fukunaka et al. [27] and Motoyama et al. [28]. Table 1 summarizes the calculated surface pH values.

The Pourbaix diagram suggests the precipitation of Co $(OH)_2$ above pH 6.2. The calculated surface pH value exceeds 7.7 at the bulk pH value of 3.5 and 6.0. Thus, the precipitation of $Co(OH)_2$ is expected near the cathode surface in the electrolyte solution with pH 6.0, and even

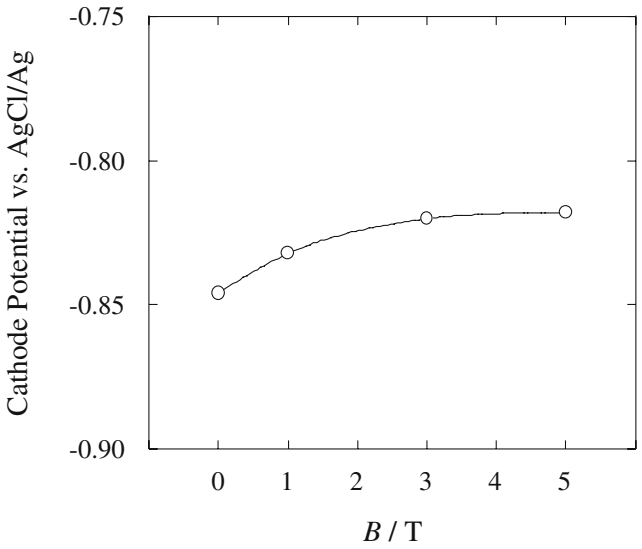

Fig. 7 Cathode potential measured at various magnetic field intensities during cobalt electrodeposition at 10 mA cm^{-2} (electrolyte: 1.65 M $CoSO_4$, 0.35 M $CoCl_2$, 0.38 M H_3BO_3; pH 1.5)

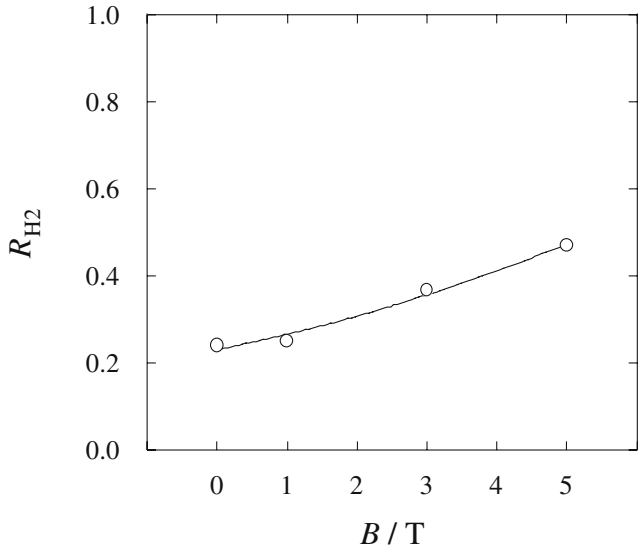

Fig. 8 Ratio of the hydrogen partial current to the total current, R_{H2}, measured at various magnetic intensities during cobalt electrodeposition at 10 mA cm^{-2} (electrolyte: 1.65 M $CoSO_4$, 0.35 M $CoCl_2$, 0.38 M H_3BO_3; pH 1.5)

3.5. In the present case, the precipitated hydroxide may be selectively adsorbed at α-Co(110). The selectivity may induce a slower growth rate of α-Co(110) and result in the preferential growth of the (100) plane. However, the XRD pattern did not show the $Co(OH)_2$ phase. To confirm the cobalt hydroxide, therefore, further surface analysis will be necessary.

Magnetic field effects

The magnetic field effect was investigated in the acidic solution (pH 1.5). The field was superimposed perpendicular to the electric field to generate the upward MHD convection as indicated in Fig. 1.

The deposition potential is plotted for the various magnetic flux intensities in Fig. 7. It shifts toward the anodic direction with increasing the field intensity, which is caused by MHD convection. The Kyoto University research team (Iida et al. submitted for publication) has conducted water electrolysis in the magnetic field and measured the ohmic resistance drop between the working and reference electrode. The MHD convection improves the electrode surface coverage by removing the gas bubbles sticking to the electrode surfaces and reduces the void fraction in the electrolyte-bubble dispersion zone because the convection considerably stirs the electrolyte in the vicinity of the electrode. Therefore, the ohmic resistance is smaller in the magnetic field so that the electrode potential should shift toward the anodic direction.

The hydrogen gas evolution ratio, R_{H2}, increases to about 50% with increasing magnetic field intensity, as shown in Fig. 8. The phenomenon agrees well with the results for the

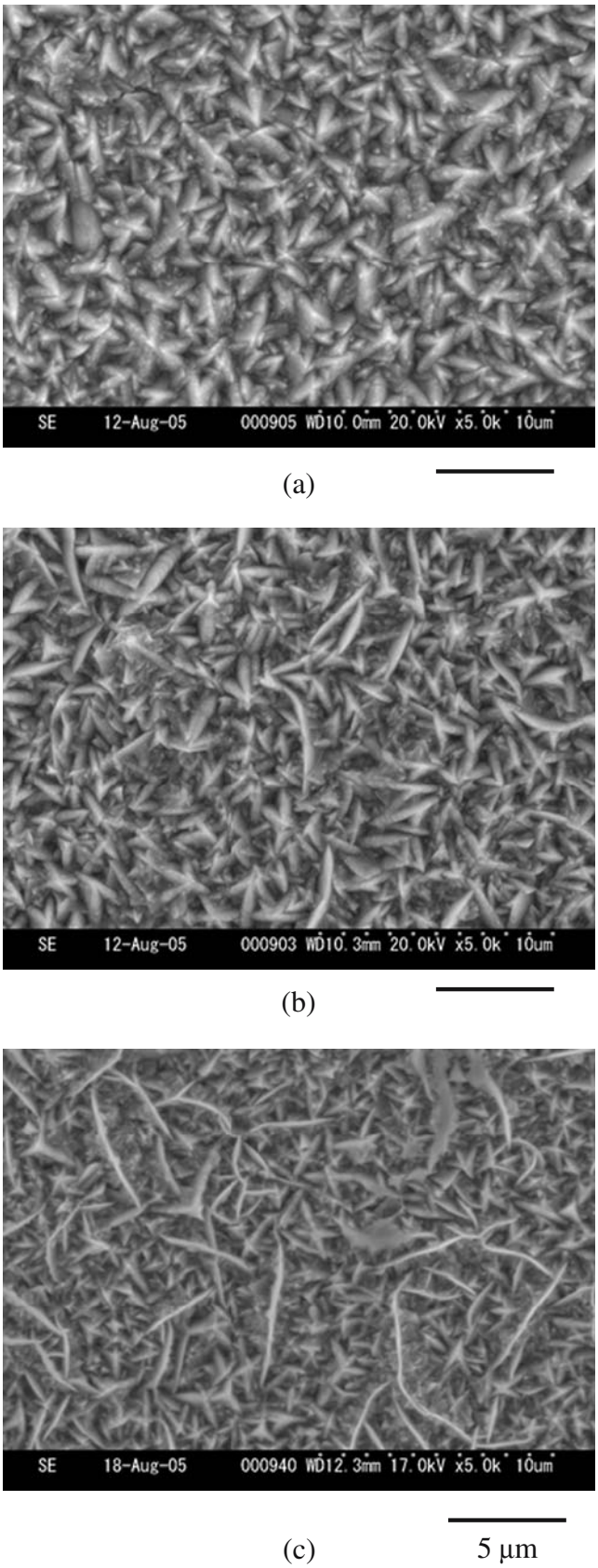

Fig. 9 SEM images of the cobalt surface morphology electrodeposited at 10 mA cm^{-2} with 150 C cm^{-2} in pH 1.5 [B=0 T (**a**), 3 T (**b**), and 5 T (**c**)]

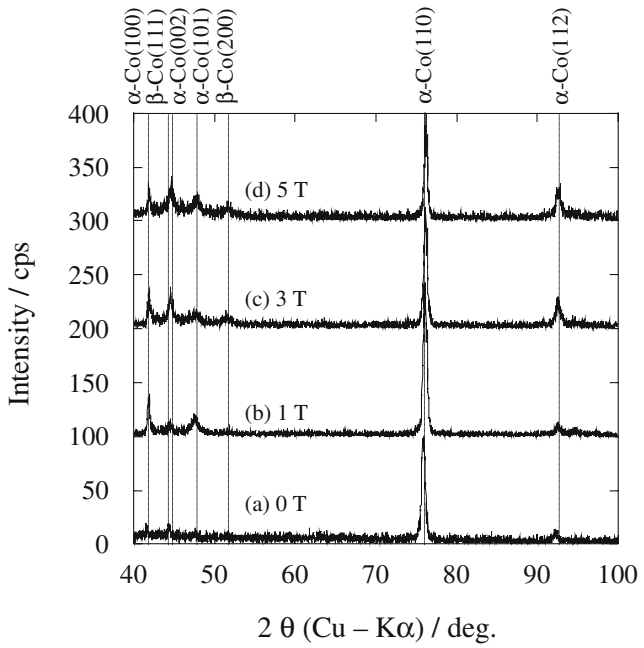

Fig. 10 XRD patterns of the cobalt film electrodeposited at 10 mA cm^{-2} in various magnetic field intensities, B=0 T (**a**), 1 T (**b**), 3 T (**c**), and 5 T (**d**) (pH 1.5, 150 C cm^{-2})

electrodeposition of ferromagnetic metals (Fe [16] and Ni [29]). The surface concentration of H^+ ion is smaller than the bulk concentration due to the consumption of the H_2 gas evolution reaction [27, 28]. In a magnetic field, MHD convection can enhance the ionic mass transfer rate of H^+ toward the cathode surface. The equilibrium potential of the hydrogen evolution shifts to the anodic direction, which results in a higher rate of hydrogen gas evolution, i_{H2}.

The cobalt film was electrodeposited under the electrolytic condition of 10 mA cm^{-2} and pH 1.5 to examine the effect of a magnetic field on the surface morphology. Figure 9 shows the SEM images of Co film electrodeposited at (a) 0 T, (b) 3 T, and (c) 5 T, respectively. The figure demonstrates no drastic morphological variations with the magnetic flux intensity. The shape of precipitates does not seem to change among three SEM images, but some grains with an elongated ridge-shape preferentially appear in the pyramidal precipitates matrix with increasing magnetic flux intensity. It corresponds well with our previous work [30].

Figure 10 presents the XRD patterns obtained in various magnetic flux intensities. Although the strongest peak of α-Co(110) is maintained as seen in Fig. 5, the peaks of α-Co(100) and α-Co(101) appear in the magnetic field. Moreover, in the high magnetic field (>3 T), β-Co(200) cubic line appears at 52° and the diffraction intensity slightly increases with increasing the magnetic field intensity. The peak around 45° also grows beyond 3 T. Because the peak consists of the diffraction of α-Co(002) (44.76°) and β-Co(111) (44.25°), it will be possible to calculate the ratio of α-Co crystalline to β-Co by using the pole figure measurement as reported by Armyanov and Vitkova [31].

It has been reported that β-Co crystalline is formed when the hydrogen gas evolution is active [22, 25]. Similar to our experiment, β-Co is probably formed by the high rate of the hydrogen evolution that is surely promoted by the MHD convection as shown in Fig. 8. The rate of the atomic hydrogen incorporation might be proportional to the hydrogen evolution rate. That is, the high rate of the hydrogen incorporation in a magnetic field could form the metastable cobalt hydride, which might facilitate the β-Co formation [25].

Conclusions

Cobalt electrodeposition from a $CoSO_4$ solution was investigated from the viewpoints of two factors, pH and magnetic field.

pH Effect The deposition potential slightly shifted toward the anodic direction with increasing pH value (pH 1.5–6.0). The surface morphology drastically changed from pyramidal (pH 1.5) to large-sized flattened precipitates (pH 6.0). While the strongest peak of α-Co(110) was maintained over the range of pH 1.5–3.5, the preferential growth of the α-Co(100) crystalline plane was promoted probably due to the hydroxide adsorption on the α-Co(110) plane.

Magnetic field effect The effect of a magnetic field on the electrodeposited Co film was examined at pH 1.5. The deposition potential slightly shifted toward the anodic direction with increasing the magnetic field intensity because MHD convection decreased the ohmic resistance by the existence of a gas bubble-dispersion layer. In higher magnetic fields (>3 T), grains with an elongated ridge shape appeared in the pyramidal precipitates matrix. Moreover, β-Co was formed with the enhancement of the hydrogen evolution. The formation of β-Co might be caused by the acceleration of the atomic hydrogen incorporation into the electrodeposits.

Acknowledgments The authors wish to thank Prof. S. Kikuchi in Shiga Prefecture University for XRD measurements and his valuable discussion and to Dr. M. Motoyama for the calculations of the surface pH values. Part of this work was performed under the financial aid given to Y. Fukunaka by the Ministry of Education, Science and Technology (Project No. 15360402), for which the authors are grateful. One of the authors, H. Matsushima, wishes to express his sincere gratitude to the Alexander von Humboldt Foundation in Germany.

References

1. Saboungi LM, Rosso M, Peter ML (eds) (2005) Special issue of international symposium on material processing for nanostructured devices 2003. J Electroanal Chem 584
2. Plieth W (ed) (2004) Special issue of 3rd international symposium on electrochemical processing of tailored materials. J Solid State Electrochem 8
3. Ito Y, Peter L (ed) (2003) Special issue of international symposium on materials processing for nanostructured devices 2001. J Electroanal Chem 559
4. Armyanov S (2000) Electrochim Acta 45:3323
5. Cavallotti PL, Vicenzo A, Bestetti M, Franz S (2003) Surf Coat Technol 76:169–170
6. Uhlemann M, Krause A, Chopart JP, Gebert A (2005) J Electrochem Soc 152:C817
7. Motoyama M, Fukunaka Y, Kikuchi S (2005) Electrochim Acta 51:897
8. Bund A, Koehler S, Kuehnlein HH, Plieth W (2003) Electrochim Acta 49:147
9. Aogaki R, Fueki K, Mukaibo T (1975) Denki Kagaku 43:504
10. Tabakovic I, Riemer S, Sun M, Vasko VA, Kief MT (2005) J Electrochem Soc 152:C851
11. Krause A, Hamann C, Uhlemann M, Gebert A, Schultz L (2005) J Magn Magn Mater 261:290–291
12. Bund A, Ispas A (2005) J Electroanal Chem 575:221
13. Coey JMD, Hinds G (2001) J Alloys Compd 326:238
14. Fahidy TZ (2001) Prog Surf Sci 68:155
15. Matsushima H, Fukunaka Y, Ito Y, Bund A, Plieth W (2006) J Electroanal Chem 587:93
16. Matsushima H, Nohira T, Ito Y (2004) Electrochem Solid-State Lett 7:C81
17. Matsushima H, Nohira T, Mogi I, Ito Y (2004) Surf Coat Technol 179:245
18. Aizi A, Sahari A, Felloussia ML, Schmerber G, Meny C, Dinia A (2004) Appl Surf Sci 228:320
19. Valizadeh S, George JM, Leisner P, Hultman L (2001) Electrochim Acta 47:865
20. Bartlett PN, Birkin PN, Ghanem MA, DeGroot P, Sawicki M (2001) J Electrochem Soc 148:C119
21. Cheng TJ, Jorne J, Gau JS (1990) J Electrochem Soc 137:93
22. Vicenzo A, Cavallotti PL (2004) Electrochim Acta 49:4079
23. Matsushima JT, Trivinho SF, Pereira EC (2006) Electrochim Acta 51:1960
24. Cohen HT, Kaplan WD, Yahalom J (2002) Electrochem Solid-State Lett 5:C75
25. Nakahara S, Mahajan S (1980) J Electrochem Soc 127:283
26. Nakano H, Nakahara K, Kawano S, Oue S, Akiyama T, Fukushima H (2002) J Appl Electrochem 32:43
27. Fukunaka Y, Aikawa S, Asaki Z (1994) J Electrochem Soc 141:1783
28. Motoyama M, Fukunaka Y, Sakka T, Ogata HY (2006) J Electrochem Soc 153:C502
29. Wassef O, Fahidy TZ (1976) Electrochim Acta 21:727
30. Matsushima H, Fukunaka Y, Yasuda H, Kikuchi S (2005) ISIJ Int 45:1001
31. Armyanov S, Vitkova S (1978) Surf Technol 7:319